Mapping auditory nerve firing density using high-level compound action potentials and high-pass noise masking[a)]

Brian R. Earl[b)] and Mark E. Chertoff
Department of Hearing and Speech, University of Kansas Medical Center, 3031 Miller, 3901 Rainbow Boulevard, Kansas City, Kansas 66160-7605

(Received 16 December 2010; revised 20 October 2011; accepted 25 October 2011)

Future implementation of regenerative treatments for sensorineural hearing loss may be hindered by the lack of diagnostic tools that specify the target(s) within the cochlea and auditory nerve for delivery of therapeutic agents. Recent research has indicated that the amplitude of high-level compound action potentials (CAPs) is a good predictor of overall auditory nerve survival, but does not pinpoint the location of neural damage. A location-specific estimate of nerve pathology may be possible by using a masking paradigm and high-level CAPs to map auditory nerve firing density throughout the cochlea. This initial study in gerbil utilized a high-pass masking paradigm to determine normative ranges for CAP-derived neural firing density functions using broadband chirp stimuli and low-frequency tonebursts, and to determine if cochlear outer hair cell (OHC) pathology alters the distribution of neural firing in the cochlea. Neural firing distributions for moderate-intensity (60 dB pSPL) chirps were affected by OHC pathology whereas those derived with high-level (90 dB pSPL) chirps were not. These results suggest that CAP-derived neural firing distributions for high-level chirps may provide an estimate of auditory nerve survival that is independent of OHC pathology. © *2012 Acoustical Society of America*. [DOI: 10.1121/1.3664052]

PACS number(s): 43.64.Pg, 43.64.Nf, 43.64.Kc, 43.64.Ri [TD] Pages: 337–352

I. INTRODUCTION

Objective diagnostic tools such as otoacoustic emissions (OAEs) and auditory evoked potentials (AEPs) have significantly reduced the age of identification of hearing loss in children (Cone-Wesson *et al*., 2000) and enhanced differentiation of the sensory and neural components of hearing loss. Since OAEs and short-latency AEPs reflect the function of cochlear outer hair cells (OHCs) and the auditory nerve, respectively, they likely offer the best non-invasive glimpse of peripheral pathophysiology contributing to sensorineural hearing loss. Optimizing these diagnostic tools to pinpoint the cochlear location of hair cell loss and auditory nerve pathology may improve individualization of gain prescriptions for hearing aid users and mapping strategies for cochlear implant recipients. Precise diagnostic tools will also be crucial if regeneration of cochlear hair cells and auditory neurons eventually becomes a viable treatment option for hearing-impaired individuals.

Presence or absence of OAEs and threshold and latency of AEPs are the parameters commonly analyzed in the audiology clinic. However, analysis of other response parameters such as fine-structure, amplitude, response area, and waveform morphology may expand the diagnostic utility of these measures. For example, Don *et al*. (2005) demonstrated that their stacked auditory brainstem response (ABR) technique, which optimizes wave V amplitude by temporally aligning and summing derived-band ABRs, detects the presence of small acoustic neuromas with 95% sensitivity and 88% specificity. In a mouse model of temporary noise exposure, Kujawa and Liberman (2009) found that ABR amplitudes at high stimulus levels were better than thresholds at predicting auditory neuron degeneration. Ferraro and Durrant's (2006) method of calculating the area ratio between the summating potential (SP) and the action potential (AP) portions of electrocochleography waveforms achieves 92% sensitivity and 84% specificity in diagnosing Ménière's disease/endolymphatic hydrops (Al-momani *et al*., 2009). Other studies in the cochlear implant literature have indicated that the amplitude of electrically evoked auditory potentials is positively correlated with the number of viable auditory neurons (Smith and Simmons, 1983; Hall, 1990) and may gauge prognoses for implant recipients (Gibson and Sanli, 2007; Teagle *et al*., 2010).

Chertoff (2004) and Chertoff *et al*. (2008) used a gerbil model to determine the utility of the compound action potential (CAP) for quantifying auditory nerve pathology. Their approach was to analyze the morphology of CAPs by fitting the waveforms with a five-parameter convolution model adapted from Goldstein and Kiang's (1958) description of the CAP as the sum of synchronously firing auditory neurons. One of the model parameters (N) scales the amplitude of the N_1 portion of the CAP similar to conventional measures of N_1 amplitude (i.e., baseline to N_1 peak) and theoretically represents the number of nerve fibers contributing synchronously to the recorded response.

Earl and Chertoff (2010) tested this theory by using the convolution model to fit CAPs evoked with tonebursts (1–16 kHz) in gerbils with partial lesions of the auditory nerve. At high stimulus levels (100 dB SPL for 1–8 kHz,

[a)]Portions of this work were presented at the 33rd and 34th Midwinter Meetings of The Association for Research in Otolaryngology, Anaheim, CA, February 2010; Baltimore, MD, February 2011.
[b)]Author to whom correspondence should be addressed. Electronic mail: bearl@kumc.edu

75 dB SPL for 16 kHz), the model parameter N was positively correlated with the percentage of surviving nerve fibers within the whole nerve bundle. The strength of correlation (r) reached 0.87 for 1 kHz stimuli suggesting that the amplitude of high-level CAPs could reliably predict overall auditory nerve survival. The corresponding cochlear location of neural survival, however, could not be determined by analyzing amplitude values across stimulus frequency, which is consistent with the broad displacement patterns that high-level toneburst stimuli generate on the basilar membrane (Eggermont, 1976; Russell and Nilsen, 1997).

A location-specific estimate of neural survival may be possible using a masking paradigm to systematically limit the region of auditory neurons contributing to high-level CAPs. The schematic of an uncoiled cochlea in the top panel of Fig. 1 and the accompanying plots [Figs. 1(b) and 1(c)] illustrate the theory behind the high-pass masking technique explored in this study. A high-level stimulus that triggers synchronous neural excitation along a large portion of the cochlea (e.g., broadband chirp) is used to evoke CAPs while the high-pass cutoff frequency of simultaneous masking noise is stepped from low frequencies encoded in the apex to high frequencies encoded in the base. Preliminary experiments in normal-hearing animals indicated that N_1 amplitude increases in a sigmoid manner as progressively more neurons are allowed to contribute to chirp-evoked CAPs [solid line in Fig. 1(b)]. Plotting the derivative of the cumulative amplitude growth function yields a neural density function that is hypothesized to represent the spread of neural firing generated in the cochlea by a given stimulus [solid line in Fig. 1(c)]. In a cochlea with a gap of missing auditory nerve fibers [dashed line in Fig. 1(b)], normalized N_1 amplitude

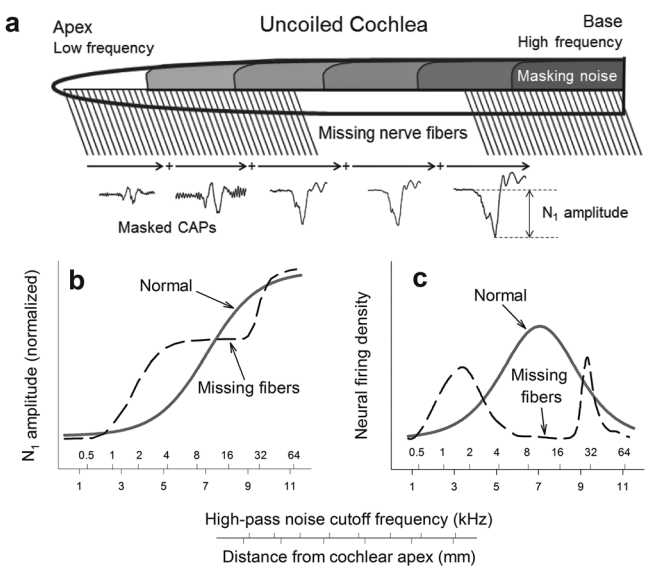

FIG. 1. (a) Schematic of an uncoiled cochlea illustrates the idea of using multiple bandwidths of high-pass noise to systematically limit the region of auditory nerve fibers that can contribute synchronously to CAPs evoked with high-level stimuli. (b) N_1 amplitude (normalized relative to the unmasked N_1 amplitude) would theoretically grow differently for a cochlea with missing auditory nerve fibers (dashed line) than for a normal cochlea (solid line). (c) Derivatives of the respective amplitude growth functions yield density functions that theoretically reveal the distribution of viable nerve fibers contributing to the CAP.

would increase relatively faster than normal until the masker cutoff frequency moves into the region of missing nerve fibers. Without additional nerve fibers to contribute to the CAP, the amplitude function would plateau until the masker moves basally to the location where nerve fibers are present. The neural density function for the cochlea with missing fibers [dashed line in Fig. 1(c)] would show a drop in neural firing density that is hypothesized to identify the distance along the cochlear partition where neurons are nonfunctional or absent. Regions of surviving neurons [e.g., apex and base of cochlea in Fig. 1(a)] would show an increase in neural firing density relative to normal [e.g., left and right portions of dashed line in Fig. 1(c)] because the surviving fibers would account for a relatively larger than normal portion of the neural density function.

The theory that CAP-derived neural density functions can predict the corresponding cochlear location of auditory nerve pathology will be tested in a future study using an animal model of partial auditory nerve degeneration. The objectives of this preliminary study were to

(1) Use the high-pass masking technique to establish normative ranges for CAP-derived neural density functions.
(2) Determine if OHC pathology alters neural density functions.

Normative ranges for CAP-derived neural density functions were established using two different acoustic stimuli at a high level (90 dB pSPL) and a moderate level (60 dB pSPL) in a group of normal-hearing gerbils (experiment 1). First, a broadband chirp stimulus was hypothesized to be the ideal stimulus for mapping neural firing density throughout the majority of the cochlea. By sweeping the instantaneous frequency from low to high frequencies at a rate that is inversely related to the traveling wave delay, a chirp stimulus theoretically generates broad, in-phase displacements of the basilar membrane and synchronous neural firing. Physiologic evidence for this theory was provided by Shore and Nuttall (1985) who observed that low-level CAPs evoked in guinea pig with rising frequency chirps were significantly larger in amplitude and had narrower waveform morphology than those evoked with falling-frequency chirps or clicks. In a recent study in human participants with a similar experimental design, Chertoff *et al.* (2010) also found that rising-frequency chirps evoked larger CAPs than both falling-frequency chirps and traditional click stimuli of equivalent magnitude and spectral bandwidth.

The second type of stimulus chosen for experiment 1 was a high-level 2 kHz toneburst (relatively low frequency for gerbil). The spectrum of a 2 kHz toneburst contains only a fraction of the spectral energy of a broadband chirp, but several studies (e.g., Eggermont, 1976; Eggermont *et al.*, 1976; Russell and Nilsen, 1997; Ren and Nuttall, 2001; Overstreet *et al.*, 2002) suggest that high-level low frequency stimuli produce a substantial spread of excitation along the cochlear partition. For example, Eggermont (1976) used a high-pass masking protocol to infer the neuronal response area contributing to CAPs evoked in guinea pig with 2 kHz tonebursts. At a moderately high level of 73 dB SPL, narrowband CAP amplitudes indicated that 2 kHz tonebursts

produced neural excitation that spanned nearly four octaves from the 0.8 to 12 kHz place of the guinea pig cochlea. More importantly, measurements of basilar membrane velocity in the basal region of gerbil cochlea by Ren and Nuttall (2001) and Overstreet *et al*. (2002) indicate linear, in-phase displacements for stimulus frequencies an octave or more below the characteristic frequency which theoretically enhances synchrony of neural firing (Békésy, 1960). There is an approximate 20-dB drop in the magnitude of basilar membrane velocity for high-level stimuli (e.g., 90 dB SPL) at frequencies an octave or more below the characteristic frequency (Ren and Nuttall, 2001), but the common observation that the latency of high-level low frequency CAPs is nearly equivalent to the latency of high-level high frequency CAPs (e.g., Chertoff, 2004) suggests that high-level low frequency stimuli generate substantial upward activation. Although a click stimulus would be comparable to a broadband chirp stimulus in terms of its spectrum, a click was not used in this experiment because of the temporally disperse nature of its expected neural activation pattern. This temporal dispersion may result in smearing of neural contributions from neighboring cochlear regions that could confound the interpretation of the cumulative growth of CAP amplitude.

The effect of OHC pathology on high-level neural density functions was determined in a subsequent experiment (experiment 2) by comparing high-level and moderate-level neural density functions obtained from gentamicin-exposed gerbils to the normative ranges established in experiment 1. The findings of Dallos and Harris (1978), Ruggero and Rich (1991), and Fridberger *et al*. (2002) suggest that OHCs act primarily to enhance basilar membrane displacement for low to moderate-level inputs. High-level inputs (e.g., 90 dB SPL) are assumed to trigger basilar membrane displacement that is large enough to stimulate the inner hair cells (IHCs) directly. Therefore, any changes in high-level neural density functions would not be related to OHC pathology but would reflect the status of the primary afferent neurons and/or the IHCs with which they synapse. Neural density functions for moderate-level stimuli (e.g., 60 dB SPL) would be expected to be influenced by OHC pathology.

II. MATERIALS AND METHODS

A. Animal preparation

Young-adult Mongolian gerbils (Meriones unguiculates), weighing between 45 and 70 g, were used for this study. Prior to surgery, all animals were sedated with an initial intraperitoneal injection of pentobarbital (64 mg/kg). Supplementary intramuscular injections of pentobarbital (~30 mg/kg) were given hourly to maintain appropriate sedation throughout the surgery and data collection. Animals were placed in the supine position and wrapped in a warming pad to maintain body temperature at 37 °C. Following local injection of lidocaine, a 10–15 mm post-auricular incision was made and the underlying neck musculature was dissected to access the right middle ear cavity (bulla). The bulla was opened with surgical tweezers to allow for placement of an electrode in the round window niche for CAP recordings (experiments 1 and 2) and delivery of gentamicin solution to the niche to induce OHC impairment (experiment 2). All experimental procedures were approved by the Institutional Animal Care and Use Committee of the University of Kansas Medical Center.

B. Generation of CAP stimuli and masking noise

A broadband chirp stimulus and a 2 kHz toneburst stimulus (1 ms rise/fall times, 8 ms plateau) were generated for this study. The chirp stimulus [Fig. 2(a)] was tailored to gerbil by sweeping the frequency from 1 to 60 kHz at a rate that coincides with the inverse of the cochlear traveling wave delay in gerbil [Fig. 2(b)]. The cochlear traveling wave delay was estimated by fitting gerbil CAP latency data for toneburst stimuli between 1 and 16 kHz at 5 dB above threshold (Earl and Chertoff, 2010) with the following equation of Anderson *et al*. (1971):

$$t(f) = cf^{\alpha}, \tag{1}$$

where $t(f)$ is cochlear traveling wave delay in seconds (s), f is stimulus frequency in Hz, and the constants c and α are 0.01415 and −0.1960, respectively. Using these constants and equations (3)–(6) of Fobel and Dau (2004), the chirp waveform was generated in MATLAB (MathWorks, Natick, MA) using a time resolution of 4 μs (i.e., sampling frequency = 250 kHz). Ramping up the amplitude of the chirp stimulus [Fig. 2(a)] as the instantaneous frequency increased, according to the amplitude scaling factor of Fobel and Dau (2004) [Eq. (7)], produced a chirp with relatively flat spectral magnitude between 1 and 60 kHz [Fig. 2(c)]. The effect of the amplitude scaling factor on the instantaneous frequency of the resultant chirp was negligible (normalized root-mean-square deviation between instantaneous frequency of the unscaled-chirp and that of the scaled-chirp was 0.3%).

The chirp stimuli were presented at a rate of 25 per s and the 2 kHz tonebursts were presented at a rate of 40 per s. A relatively long-duration (10 ms) toneburst was chosen to facilitate differentiation of the N_1 and SP components of the CAP. Both stimuli were delivered with alternating polarity to minimize the presence of the cochlear microphonic (CM) in the CAP waveform. Although alternating polarity stimuli are expected to temporally smear neural firing at the level of single units, they have not been shown to influence the latency of a compound neural response such as the CAP (Don *et al*., 1996).

Broadband white noise was generated (digital-to-analog sampling rate = 97.7 kHz) and high-pass filtered with a fifth-order "Biquad" filter (slope ≥ 80 dB per octave) using signal processing software (RPvdsEx) and a real-time processor (RP2) from Tucker-Davis Technologies (TDT; Alachua, FL). Multiple high-pass cutoff frequencies were chosen to correspond to 0.25 mm increments along the first 3 mm of the base of the gerbil cochlea where the best frequency ranges from 62.8 kHz to 15.6 kHz. For the middle through apical regions of the gerbil cochlea (3–11 mm), where the best frequency ranges from 14.8 kHz to 150 Hz, cutoff frequencies were chosen to correspond to 0.5 mm increments. The lowest cutoff frequency was 400 Hz and the highest cutoff frequency was 45 987 Hz making a total of 25 masking conditions. Higher cutoff frequencies (i.e., greater than 50 kHz) were not possible due to the sampling-rate limitation of the real-time processor.

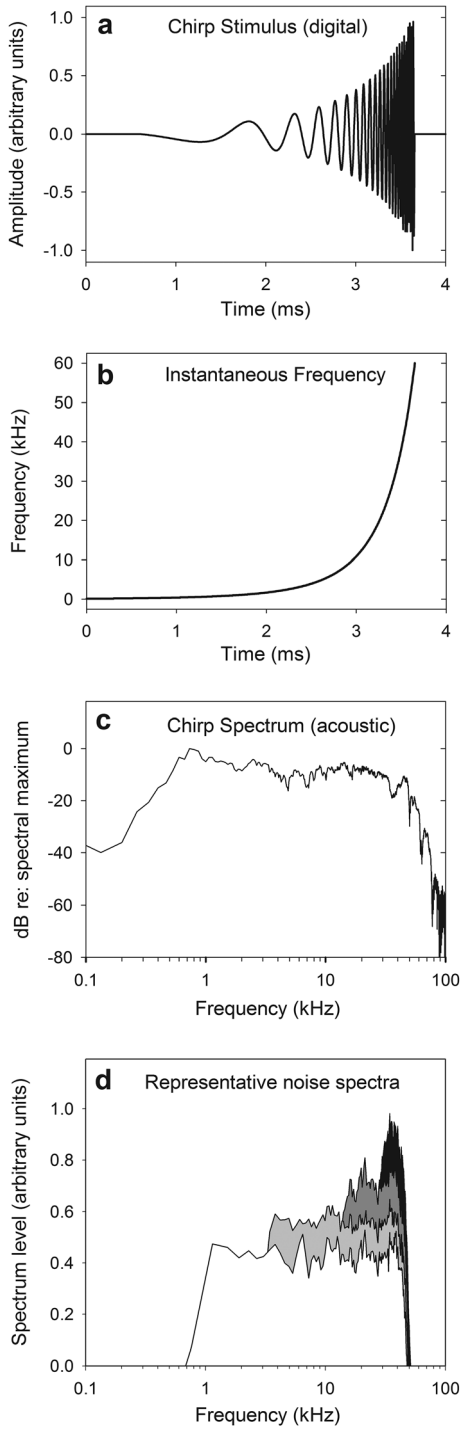

FIG. 2. (a) Digital waveform of gerbil-tailored chirp stimulus rising in frequency and amplitude over a duration of 3.06 ms. (b) Instantaneous frequency of chirp stimulus is equivalent to the inverse of cochlear traveling wave delay in gerbil (estimated with gerbil CAP latency data from Earl and Chertoff, 2010). (c) Acoustic spectrum of chirp stimulus shows relatively flat spectral energy between 1 and 60 kHz, spanning nearly the entire range of gerbil hearing. (d) Representative spectra of four of the high-pass masking conditions illustrating the increase in spectrum level to equalize the rms SPL across all conditions.

The root-mean-square (rms) level of each masking condition was equated to the rms SPL of the masking condition with the broadest noise bandwidth (i.e., 0.4–50 kHz). The necessary increase in magnitude (i.e., correction factor in dB) as a function of masker cutoff frequency followed a third-order polynomial trend that reached 17 dB for the highest cutoff frequency of 45 987 Hz [see representative spectra in Fig. 2(d)]. An energy equalization approach was used to ensure that progressive decreases in the spectral energy of the masking noise were not responsible for the cumulative growth of CAP amplitude. This approach is different than the high-pass masking paradigms used in other studies (e.g., Teas *et al.*, 1962; Don *et al.*, 1979) that held constant the spectrum level of different masker bandwidths. However, within-animal comparisons between the traditional approach (i.e., spectral level equalization) and the approach used in this study (i.e., spectral energy equalization) revealed that both approaches resulted in essentially equivalent CAP amplitude growth functions for high-level chirp stimuli. This observation suggests that, despite an increase in masker level by up to 17 dB, the steepness of the high-pass filter slopes and the mechanical damping inherent in the cochlea (approximately 90 dB/octave toward the apex) essentially restrict the spread of the masker to the cochlear region bounded by the place corresponding to the cutoff frequency and the place corresponding to the high-frequency limit of the masking noise.

The masking noise was added to the CAP stimulus (chirp or 2 kHz toneburst) with a signal mixer (SM5, TDT) and delivered free-field via a magnetic loudspeaker (FF1, TDT) with a relatively flat (+/− 8 dB) frequency response from 1 to 50 kHz. Electromagnetic artifact from the loudspeaker was minimized to negligible levels by housing the loudspeaker in a custom-made mu metal case (MμShield; Manchester, NH) and by positioning it 15 cm away from the right pinna of the animal. A 1/8 in. Brüel & Kjaer (Denmark) microphone (B&K 4138) was suspended within 5 mm of the ear canal opening and at a 90° azimuth relative to the diaphragm of the loudspeaker. The reported frequency sensitivity of the B&K microphone is essentially flat (+/− 2 dB) from 0.02 to 100 kHz when it is positioned at a 90° azimuth relative to the sound source. The microphone output was routed to an oscilloscope (Tektronix, TDS 2014) to calibrate the peak SPL (pSPL) of the stimulus, and to a spectrum analyzer (Hewlett Packard, 3561 A) to verify the spectral bandwidth of the noise during each masking condition.

C. CAP recordings

CAPs were recorded from right cochleae using a silver ball electrode on the round window and a ground electrode in the contralateral shoulder musculature. An absorbent cotton wick (Densply Maillefer, Tulsa, OK) was placed next to the round-window electrode and subsequently changed every 15 min to control fluid build-up in the niche. The electrophysiologic signals were amplified by a factor of 5 000, band-pass filtered (0.03–6 kHz) by two amplifiers/filters in series (Stanford Research Systems SR560, Sunnyvale, CA; Stewart Electronics VBF10, Lyman, SC), and digitized at 250 kHz by an analog to digital converter (AD2, TDT) before being averaged within a 15-ms time window. A high sampling rate of 250 kHz was used because the same code interfaced with the data acquisition hardware to digitize the electrophysiologic signals and to output the chirp stimulus. Using lower sampling

frequencies could have resulted in aliasing of the chirp signal because it was designed with spectral energy from 1 to 60 kHz. Automated measurements of N_1 amplitude, computed as the voltage difference between the mean of the first ten data-points (i.e., baseline) and the minimum in the time window (i.e., N_1 trough), were displayed to the monitor in intervals of 20 averages. CAP waveforms were saved to disk after the displayed measurement of the N_1 amplitude remained relatively stable (e.g., fluctuations no greater than +/− 5%) for a minimum of 60 averages.

D. Procedures

In experiment 1, data were collected from the right ears of a group of normal-hearing gerbils ($n = 9$) to compare neural density functions for chirps and 2 kHz tonebursts at a high level (90 dB pSPL) and at a moderate level (60 dB pSPL). Animals were considered to have normal hearing sensitivity if their CAP threshold for chirps was ≤ 20 dB pSPL. N_1 amplitude growth data was obtained for the four stimulus conditions in the following order: chirps at 60 dB pSPL, 2 kHz tonebursts at 60 dB pSPL, chirps at 90 dB pSPL, and 2 kHz tonebursts at 90 dB pSPL. Each recording condition began by recording the amplitude of the N_1 component of the unmasked CAP [baseline to negative peak of N_1 as demonstrated in Fig. 3(a)]. The full-bandwidth masker (0.4–50 kHz) was then presented continuously and increased in level until the amplitude of N_1 was reduced by 80%, similar to the masking procedure of Eggermont (1977). The bandwidth of the white noise was subsequently varied by changing the high-pass cutoff frequency and CAPs were recorded for each of the 25 masking conditions. The sequence of masking conditions was randomized and interspersed with two recordings of unmasked CAPs. A fourth unmasked CAP was recorded after all masking conditions were presented. The average time required to record the 29 CAPs for one stimulus condition was 27 min while the average duration of the entire protocol of experiment 1 was just over 2 h.

The threshold for chirp-evoked CAPs was measured again at the completion of the protocol to determine if multiple presentations of masking noise led to an elevation in threshold. Early experiments in which CAP amplitude was completely masked (i.e., 100% amplitude reduction) resulted in significant increases in CAP threshold (> 10 dB) following completion of all masked recordings. This apparent over-masking and the goal of ensuring a CAP response was present during all masking conditions influenced the decision to use 80% amplitude reduction as the initial masking level. No attempts were made to measure or control for the possible effects of the middle ear reflex or the efferent nervous system on the masked-CAP recordings. Any effect of the efferent nervous system would theoretically be obscured by middle ear reflex activation by the moderate to high stimulus levels used in this study. The middle ear reflex, however, has also been shown to be essentially abolished in other rodents (e.g., rabbit; Borg and Moller, 1975) by sodium pentobarbital, the anesthetic used during all experiments in this study.

In experiment 2, data were collected from the right ears of a group of gentamicin-exposed gerbils ($n = 10$) to compare neural density functions obtained from animals with impaired OHCs to the neural density functions obtained from the normal-hearing gerbils in experiment 1. Gentamicin, an aminoglycoside antibiotic, was chosen for this study based on data from several studies indicating that OHCs are more prone to gentamicin ototoxicity than are IHCs (e.g., Wanamaker *et al.*, 1998; Heydt *et al.*, 2004). The chosen dosage of gentamicin (200 μg applied directly to the round window) was based on data for mice (Heydt *et al.*, 2004) and gerbils (Wanamaker *et al.*, 1998; Sheppard *et al.*, 2004; Suryadevara *et al.*, 2009) showing that similar dosages led to OHC pathology in the base to middle regions of the cochlea. A 200 μg/μl gentamicin solution was prepared by dissolving gentamicin sulfate powder (Sigma; St. Louis, MO) in distilled water after the manner described by Husmann *et al.* (1998). Specifically, to achieve a 200 μg/μl (i.e., 200 mg/ml) concentration of gentamicin in solution, 313 mg of gentamicin sulfate powder, containing 0.639 mg of gentamicin per mg, was dissolved in 1 ml of distilled water.

Prior to gentamicin exposure, baseline CAP thresholds were determined for chirps and toneburst stimuli at 2, 4, 8,

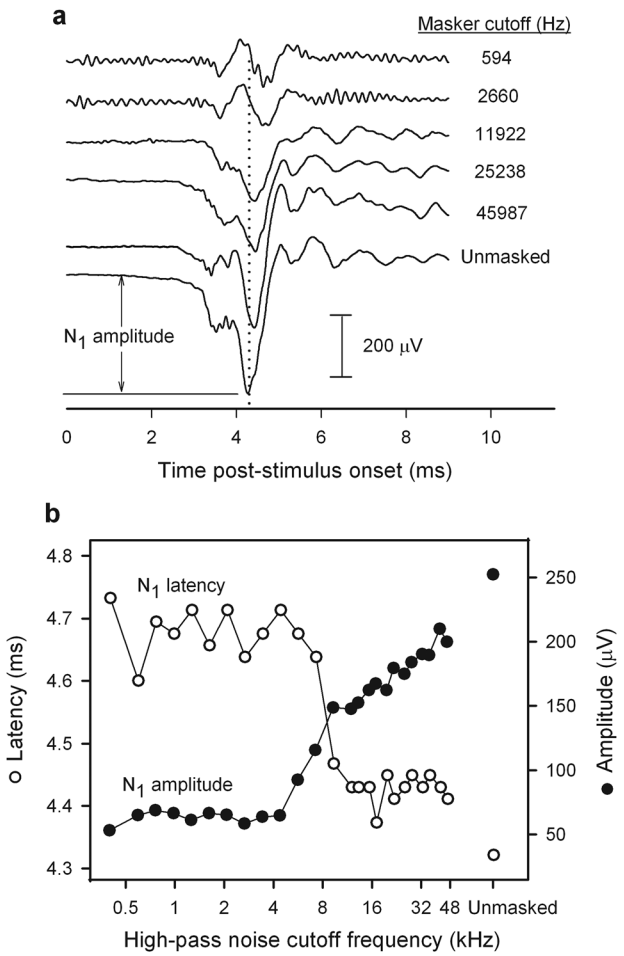

FIG. 3. (a) Representative unmasked and masked CAP waveforms for chirp stimuli at 90 dB pSPL from a normal-hearing gerbil illustrate the trend of decreasing N_1 amplitude and increasing N_1 latency as the high-pass noise masker cutoff frequency decreases. (b) Representative raw data for N_1 amplitude (filled circles, units on right ordinate) and N_1 latency (open circles, units on left ordinate) for all 25 masking conditions. Unmasked values represent the mean of four unmasked CAP recordings.

16, and 32 kHz. The amplitude of the cochlear microphonic (CM) to a 16 kHz toneburst (10 ms duration) at 80 dB pSPL was also measured prior to gentamicin delivery and then monitored during the exposure period to gauge the effect of gentamicin on OHC function. The CM recordings were acquired with the same electrode montage, recording parameters, and instrumentation set-up as the CAP recordings with one exception: the low-pass filter setting was changed from 6 to 25 kHz to capture the CM to the 16 kHz tone. A 16 kHz tone was chosen for CM monitoring because the 16 kHz-place in gerbil cochleae is in close proximity to the round window, thus providing an early indication of OHC impairment resulting from the diffusion of gentamicin through the round window membrane and into the 16 kHz region of the cochlea.

Without removing the recording electrode, 1 μl of the 200 μg/μl gentamicin solution was applied directly to the round window niche of the right cochlea. The amplitude of the CM was monitored 1 min post-gentamicin application and then in 5-min increments until the CM amplitude had dropped by at least 50% (relative to the pre-gentamicin amplitude) and at least 15 min had elapsed. The gentamicin solution was then removed from the niche with an absorbent cotton wick and the CAP threshold to chirps was measured again. If the chirp CAP threshold had increased by at least 10 dB, the experiment proceeded with measures of N_1 amplitude growth for chirps at 60 dB pSPL and then for chirps at 90 dB pSPL using the same masking procedures described above. Masked CAPs were not recorded from the gentamicin-exposed animals for 2 kHz tonebursts at 60 or 90 dB pSPL per the results of experiment 1 (see below). The chirp CAP threshold and toneburst CAP thresholds were measured again following the completion of all masked CAP recordings. The average time required for one stimulus condition (e.g., chirps at 60 dB pSPL) in experiment 2 was 23 min and the average duration of the entire masked CAP protocol (e.g., chirps at 60 and 90 dB pSPL) was 52 min.

E. Data analysis

Manual measures of N_1 peak amplitude (baseline to N_1 peak) and N_1 peak latency for all masked and unmasked CAPs recorded during both experiments were completed offline following data collection. The top panel (a) of Fig. 3 displays representative unmasked and masked CAPs evoked with chirps at 90 dB pSPL indicating the trend, observed in this and other studies (e.g., Teas *et al.*, 1962; Shore and Nuttall, 1985), of decreasing N_1 amplitude and increasing N_1 latency as high-pass masker cutoff frequency decreases. The oscillations visible in the CAP waveforms for the 594 and 2660 Hz masker cutoff conditions likely represent residual electromagnetic artifact from the loudspeaker and/or uncancelled cochlear microphonic responses to the masking noise. The oscillations are visible in the CAP waveforms for the 594 and 2660 Hz masker cut-off conditions but are absent in those for higher masker cut-off frequencies because the low-pass cutoff frequency of the secondary physiology amplifier (Stewart Electronics) was set to 6 kHz. The raw amplitude values [filled circles, Fig. 3(b)] were normalized relative to the mean amplitude of the unmasked CAPs (four unmasked recordings for each stimulus condition) to allow for amplitude growth comparisons across stimulus conditions and across animals. The raw latency values [open circles, Fig. 3(b)] were also normalized by calculating the shift in latency as the difference between the average unmasked latency and the masked latencies.

Figure 4 demonstrates the data-fitting procedure [panel (a)] and the two dependent variables used for statistical analyses [panel (b)] using representative data for high-level chirp-evoked CAPs. First, normalized N_1 amplitude values were plotted as a function of distance from cochlear apex in mm [Fig. 4(a)]. The high-pass cutoff frequencies [as shown on the abscissa of Fig. 3(b)] were converted to distance from cochlear apex in mm [as shown on the abscissa of Fig. 4(b)] using the frequency-place map for gerbil cochleae from Müller (1996). The cumulative amplitude function [CAF; thick curve in Fig. 4(a)] was obtained for each stimulus condition by using SigmaPlot (Systat Software, Inc., San Jose, CA) to fit the normalized N_1 amplitude data with the following four-parameter sigmoid function:

$$CAF(x) = y_0 + \left(\frac{a}{1 + e^{-[(x-x0)/b]}}\right), \tag{2}$$

where a scales the inflection point of N_1 amplitude growth, b governs the rate of amplitude growth, $x0$ is the distance from cochlear apex (mm) at which amplitude growth begins to inflect, and $y0$ defines the starting amplitude reduction relative to the unmasked amplitude. The parameter $y0$ is a constant in terms of Eq. (2) and in the design of the masking paradigm since the target level for the initial masked condition was 20% of the unmasked amplitude. The neural density function [NDF; thick curve in Fig. 4(b)] was obtained for each stimulus condition by using the CAF parameters to solve the analytical derivative of Eq. (2) for distance from cochlear apex (x) which is

$$NDF(x) = \left(\frac{ae^{[(x0+x)/b]}}{b\left(e^{(x0/b)} + e^{(x/b)}\right)^2}\right), \tag{3}$$

where a and b scale the peak density and bandwidth, respectively, and $x0$ is the peak location in distance from cochlear apex (mm).

The two dependent variables chosen for statistical analysis were NDF bandwidth and NDF peak location. NDF bandwidth quantifies the cochlear spread of synchronous neural firing and NDF peak location identifies the location along the cochlear partition where neural firing density reaches its peak. NDF bandwidth was defined as the distance spanned by the inner 2/3 of the area under the NDF curve and was calculated by multiplying the peak density of the NDF by 0.3413 and finding the difference between the corresponding values for distance from cochlear apex. NDF peak location was given by the value of parameter $x0$. Paired samples t-tests were used to compare bandwidth and peak location across stimulus type at 60 and 90 dB pSPL in experiment 1. Independent samples t-tests were used to compare bandwidth and peak location of chirp-generated NDFs

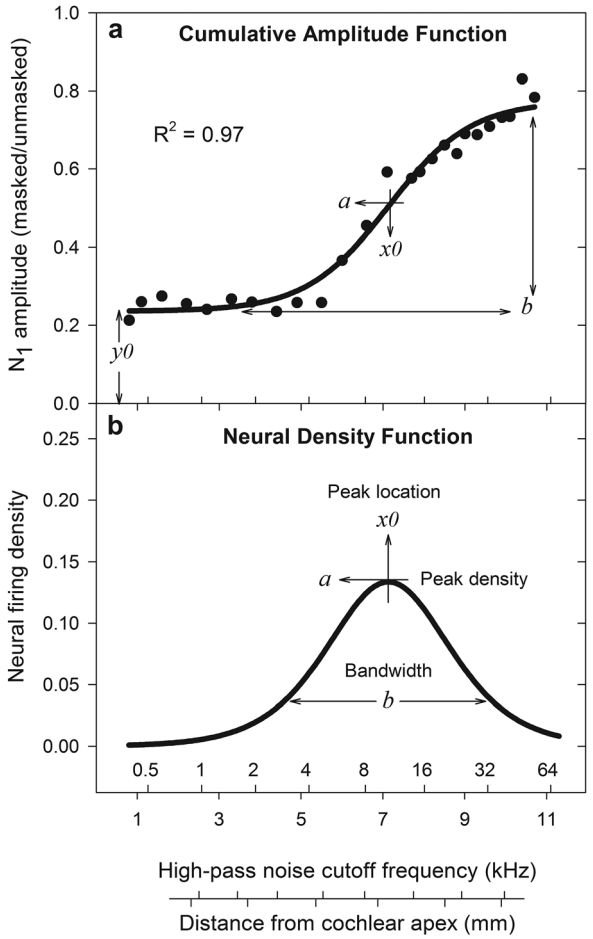

FIG. 4. (a) Representative N_1 amplitude data for CAPs evoked with chirps at 90 dB pSPL (filled circles) plotted as a function of distance from cochlear apex (transformed from high-pass noise cutoff frequency with the frequency-place map for gerbil from Müller, 1996). Fitting the N_1 amplitude data with a four-parameter (a, b, $x0$, $y0$) sigmoid function yields a cumulative amplitude function (CAF), shown with thick line along with its corresponding coefficient of determination (R^2). (b) The neural density function (NDF) (thick line) is obtained by using the CAF parameters to solve the analytical derivative of the CAF equation [Eq. (2)] for distance from cochlear apex (x). The peak location is given by parameter $x0$ and the bandwidth is defined as the distance spanned by the inner 2/3 of the area under the curve (calculated by multiplying peak density by 0.3413 and finding the difference between the corresponding distance values).

across the normal-hearing and gentamicin-exposed groups in experiment 2.

III. RESULTS

The presentation of results will focus on NDF bandwidth and NDF peak location as the two primary dependent measures of neural firing density across stimulus types in experiment 1 and across normal-hearing and gentamicin-exposed groups in experiment 2. The unmasked CAP amplitude data are also presented at the outset to demonstrate the differences between CAPs evoked with chirps and those evoked with 2 kHz tonebursts.

A. Unmasked CAP amplitudes

Representative CAPs evoked in normal-hearing gerbils with 2 kHz tonebursts and chirps at 60 dB pSPL are shown in Fig. 5(a) and Fig. 5(b), respectively. In addition to being nearly 10 times larger in magnitude than the 2 kHz toneburst CAP [Fig. 5(a)], the chirp CAP [Fig. 5(b)] has narrower N_1 morphology. Comparing the unmasked N_1 amplitudes across stimulus type and stimulus level [Fig. 5(c)] indicates that CAP amplitude increased as the stimulus intensity increased from 60 to 90 dB pSPL for 2 kHz tonebursts. For chirps, however, CAP amplitude peaked at 60 dB pSPL. Remarkably, chirps at 30 dB pSPL ($n = 4$) generated larger CAPs than 2 kHz tonebursts at 90 dB pSPL.

The variability of unmasked CAP amplitude within animals, which served as the reference for amplitude normalization, was determined by calculating the coefficients of variation (CV) (standard deviation/mean) for the amplitude of the four unmasked CAPs recorded from each animal during each stimulus condition. The maximum, mean, and minimum CVs for each stimulus condition are displayed in Table I. The highest within-animal CV of 0.216 was observed for the unmasked amplitudes of CAPs to chirps at 90 dB pSPL from a normal-hearing gerbil. The lowest within-animal CV of 0.005 was seen for the unmasked amplitudes of CAPs to chirps at 60 dB pSPL, also from a normal-hearing gerbil. The mean CV across conditions was generally near or below 0.10, the target criterion for amplitude stability for both experiments.

B. Experiment 1: Normal-hearing group

1. Cumulative amplitude functions (CAFs)

Figure 6 shows the normalized N_1 amplitude growth data (thin lines) for the nine normal-hearing gerbils in experiment

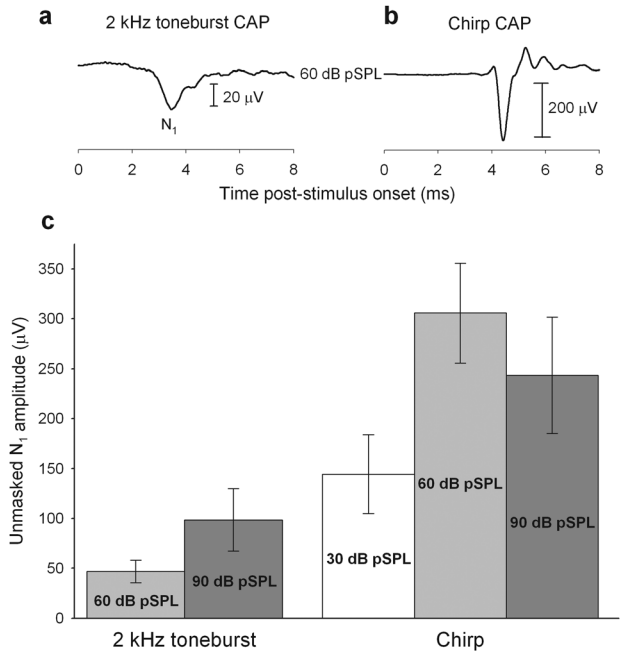

FIG. 5. A representative CAP evoked with 2 kHz tonebursts at 60 dB pSPL (a) is nearly 10 times smaller in magnitude than a CAP evoked with chirps at the same level (b). (c) Comparison of unmasked N_1 amplitudes illustrates that chirps at 60 dB pSPL produced the largest CAPs. Even chirps as low as 30 dB pSPL generated CAPs that were larger in magnitude than 2 kHz tonebursts at 90 dB pSPL. Error bars represent one standard deviation. The sample size is 9 for each stimulus condition except for the chirp condition at 30 dB pSPL for which the sample size is 4.

TABLE I. Within-animal coefficients of variation (CV) for N_1 amplitude of the four unmasked CAPs recorded from each animal during each stimulus condition.

Normal-hearing group			
	Coefficient of variation		
	Minimum	Mean	Maximum
Chirp—90 dB pSPL	0.035	0.11	0.216
Chirp—60 dB pSPL	0.005	0.036	0.098
Toneburst—90 dB pSPL	0.026	0.058	0.098
Toneburst—60 dB pSPL	0.027	0.080	0.159
Gentamicin-exposed group			
	Coefficient of variation		
	Minimum	Mean	Maximum
Chirp—90 dB pSPL	0.014	0.107	0.192
Chirp—60 dB pSPL	0.021	0.096	0.183

1 with the mean of their respective CAFs (thick lines) for chirps and 2 kHz tonebursts at 90 dB pSPL and 60 dB pSPL. The variance of the data across animals and across conditions was largest for 2 kHz tonebursts at 60 dB pSPL [Fig. 6(d)] and smallest for chirps at 60 dB pSPL [Fig. 6(c)]. The mean CAF for chirps at 90 dB pSPL [Fig. 6(a)] grows gradually and just begins to saturate near the base (i.e., 11 mm from cochlear apex). In contrast, the mean CAF for 2 kHz tonebursts at 90 dB pSPL [Fig. 6(b)] rises quickly and saturates by approximately 9 mm from the cochlear apex. The CAF for chirps at 60 dB pSPL is similar to the pattern observed for 2 kHz tonebursts at 90 dB pSPL whereas the CAF for 2 kHz tonebursts at 60 dB pSPL begins to grow near the cochlear apex and then saturates approximately 7 mm from the apex. The N_1 amplitude function depicted with the dashed thin line in panel (b) of Fig. 6 was determined to be an outlier and was excluded from statistical analysis because its initial masked amplitude was more than two standard deviations (SD) above the mean of the initial masked amplitude across all amplitude functions in experiment 1.

The mean coefficients of determination (R^2) indicate that the four-parameter sigmoid function accounts for a large majority of the variance in N_1 amplitude for all four stimulus conditions. The sigmoid function achieved the best fit for the amplitude data for chirps at 60 dB pSPL with a mean R^2 of 0.99 (range = 0.985–0.998). The lowest mean R^2 of 0.92 (range = 0.796–0.976) was observed for the fits of the amplitude data for chirps at 90 dB pSPL. The lower values and larger range for the R^2 values for the fits of the data for chirps at 90 dB pSPL was expected given the lack of a definite point of saturation for the majority of the amplitude growth functions. Accordingly, parameter a, which scales the inflection point of N_1 amplitude growth, was manually constrained for seven of the nine fits of the amplitude data for chirps at 90 dB pSPL. Without manual constraints, parameter a was not significant and the fitted function tended towards exponential growth. For each of the other three stimulus conditions, parameter a was manually constrained for only one of the nine fits. Parameter b, that governs the rate of growth of the CAF, also required manual constraints to be retained as a significant parameter and/or to preserve constant variance in three of the nine fits of the data for chirps at 90 dB pSPL and one of the nine fits of the data for 2 kHz tonebursts at 60 dB pSPL. Objectivity in choosing

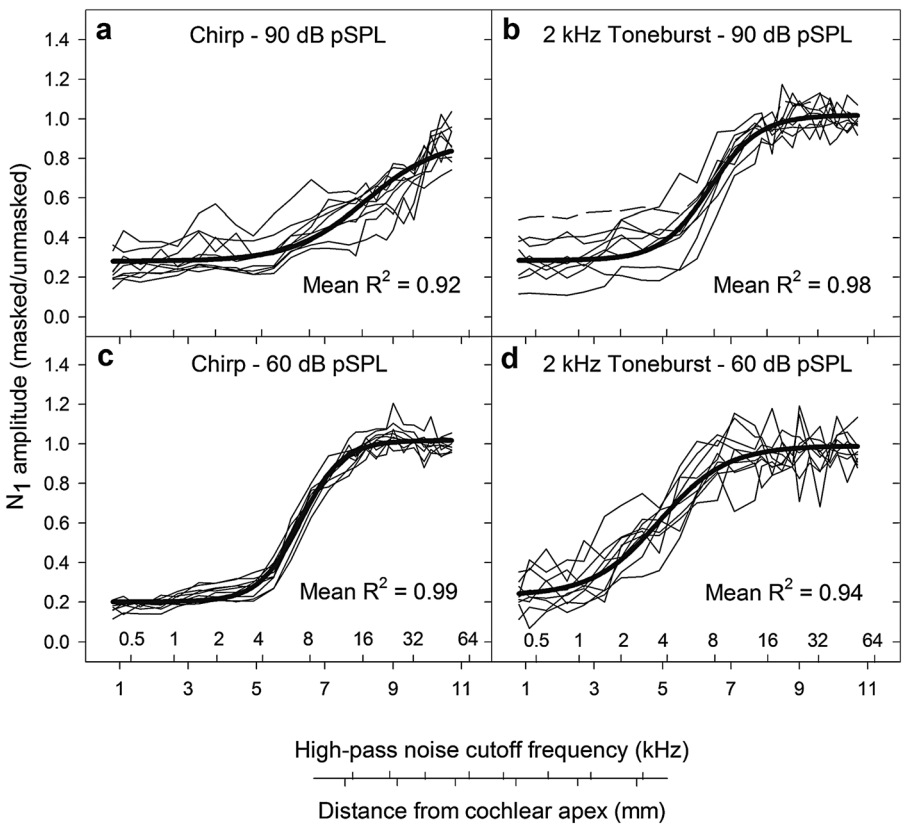

FIG. 6. Normalized N_1 amplitude growth curves (thin lines) for the nine normal-hearing gerbils (experiment 1) with their corresponding mean CAFs (thick lines) show differences in slope and variability across stimulus type and level. The amplitude growth curve shown with a dashed line in panel (b) was determined to be an outlier (i.e., initial masked amplitude was more than two SD above the mean of initial masked amplitude across all stimulus conditions) and was excluded from further analysis. Mean coefficients of determination (R^2) indicate that the four-parameter sigmoid function accounts for a large majority of the variance in the data.

manual constraints was maintained by focusing on the goal of maximizing the R^2 value while retaining significance for all four parameters.

2. Neural density functions (NDFs)

Figure 7 displays individual NDFs (thin lines), derived from individual CAFs, with their corresponding mean NDFs (heavy lines) for each of the four stimulus conditions. The NDFs illustrate, as did the CAFs, that the variance across animals was largest for 2 kHz tonebursts at 60 dB pSPL [Fig. 7(d)] and smallest for chirps at 60 dB pSPL [Fig. 7(c)]. The individual NDF shown with the dashed line in panel (b) of Fig. 7 represents the outlier that was described previously in Fig. 6.

Table II summarizes the descriptive statistics and the results of the paired samples *t*-tests used to compare the mean of the paired differences for NDF bandwidth and NDF peak location at 90 and 60 dB pSPL. At 90 dB pSPL, the mean NDF for chirps was significantly broader ($p = 0.04$) and peaked significantly closer to the base ($p = 0.001$) than the mean NDF for 2 kHz tonebursts. At 60 dB pSPL, the mean NDF for 2 kHz tonebursts was significantly broader than the mean NDF for chirps ($p = 0.04$) although the mean NDF for chirps peaked significantly closer to the base ($p < 0.001$). The assumption of normality was satisfied by the values for NDF bandwidth and NDF peak location for all four stimulus conditions in experiment 1 per Shapiro-Wilk's test of normality.

3. N_1 Latency shifts

Figure 8 displays the shift in N_1 latency (masked-unmasked latency) as a function of high-pass noise cutoff frequency across the four stimulus conditions for the nine normal-hearing gerbils (thin lines) with their respective group means (thick lines). The horizontal line at zero represents the baseline N_1 latency of unmasked CAPs. On average, the broadest bandwidth of masking noise (i.e., when the high-pass masker cutoff frequency equals 400 Hz) triggered a 0.5 ms increase in N_1 latency for the 2 kHz toneburst conditions and a 0.4 ms increase for the chirp conditions. The shift in N_1 latency remained stable across several masker cutoff frequencies before quickly decreasing to baseline N_1 latency for the high-frequency masker cutoffs. The latency shift persisted over the most masking conditions for chirps at 90 dB pSPL [Fig. 8(a)] and over the fewest masking conditions for 2 kHz tonebursts at 60 dB pSPL [Fig. 8(d)]. Similar to the trends observed in the N_1 growth data in Fig. 6, the variance across animals in N_1 latency shift was largest for 2 kHz tonebursts at 60 dB pSPL [Fig. 8(d)] and smallest for chirps at 60 dB pSPL [Fig. 8(c)]. Interestingly, the mean latency shifts (thick lines) resemble the inverse of the patterns observed for the respective mean CAFs in Fig. 6.

C. Experiment 2: Gentamicin-exposed group

1. Gentamicin-induced changes in CM amplitude and CAP threshold

The top panel (a) of Fig. 9 illustrates that the amplitude of the CM, evoked with 16 kHz tones at 80 dB pSPL, decreased exponentially over a course of minutes following application of 200 μg of gentamicin to the round window niche. Dose-response curves for gentamicin doses of 50 and 100 μg are shown for comparison. All 10 of the animals included in experiment 2 experienced at least a 50% reduction

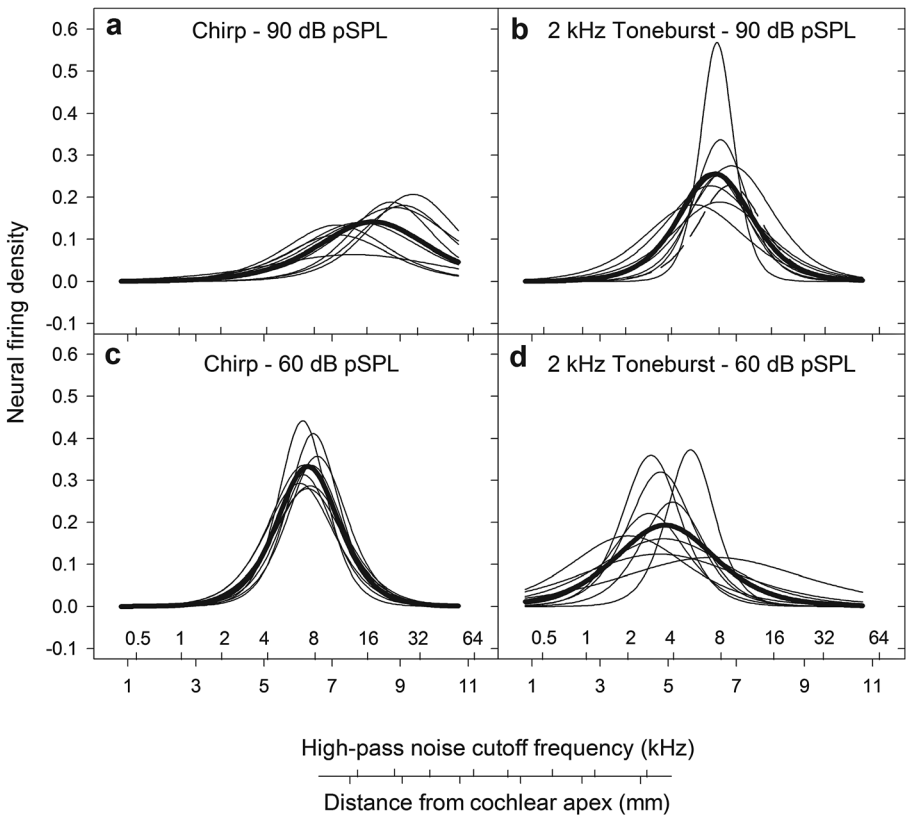

FIG. 7. Individual NDFs (thin lines) and the corresponding mean NDFs (thick lines) for the nine normal-hearing gerbils (experiment 1) illustrate the distribution of neural firing density for each stimulus type and level combination. The individual NDF shown with the dashed line in panel (b) represents the outlier that was described in Fig. 6. Statistical analyses (see Table II) indicated that the mean NDF of chirps at 90 dB pSPL was significantly broader and peaked significantly closer to the base than the mean NDF of 2 kHz tonebursts at 90 dB pSPL. At 60 dB pSPL, the mean NDF of 2 kHz tonebursts was significantly broader than the mean NDF of chirps, although the mean peak location of the chirp NDFs was significantly closer to the base than the mean peak location of the 2 kHz toneburst NDFs.

TABLE II. Descriptive statistics and results of paired samples *t*-tests comparing NDF bandwidth and peak location across stimulus type at 90 and 60 dB pSPL (experiment 1). Sample size was 8 for 90 dB pSPL conditions [due to exclusion of outlier indicated with dashed line in top right panel (b) of Fig. 6 and 9 for 60 dB pSPL conditions.

90 dB pSPL						
	Bandwidth (mm)			Peak location (mm)		
	Mean	SD[a]	*p*	Mean	SD[a]	*p*
Chirp	4.87	1.84	0.04	8.22	1.01	0.001
Toneburst	3.25			6.38		
60 dB pSPL						
	Bandwidth (mm)			Peak location (mm)		
	Mean	SD[a]	*p*	Mean	SD[a]	*p*
Chirp	2.78	2.04	0.04	6.28	0.61	< 0.001
Toneburst	4.43			4.91		

[a]SD, standard deviation of the paired differences.

in CM amplitude after an exposure to 200 μg of gentamicin lasting at least 15 min.

The bottom panel (b) of Fig. 9 shows post-gentamicin shifts in CAP thresholds for chirps (measured after removal of gentamicin from the niche) and toneburst stimuli (measured after completion of post-gentamicin masked CAP conditions). Shifts in chirp CAP thresholds ranged from 10 to 25 dB while shifts in toneburst CAP thresholds generally increased as stimulus frequency increased. Comparing the post-gentamicin measures of chirp CAP threshold to the measures of chirp CAP threshold at the completion of the post-gentamicin masked CAP conditions revealed that the largest within-animal fluctuation was 10 dB and the group mean fluctuation was less than 5 dB, indicating that threshold shifts were generally stable after exposure to gentamicin and multiple presentations of masking noise.

However, progressive elevations in CAP thresholds and steady decline in CAP amplitudes were observed in two animal experiments that began with chirps at 90 dB pSPL. Both experiments were terminated prematurely and a synergistic effect of gentamicin and noise exposure was suspected due to the high levels of masking noise required to achieve the initial 80% reduction in amplitude of the high-level CAPs. Progressive CAP threshold elevation and declining CAP amplitude were observed in only one animal experiment that started with chirps at 60 dB pSPL and consequently lower levels of masking noise.

2. CAF and NDF comparisons across groups

The top panels [(a) and (b)] of Fig. 10 compare the individual amplitude growth data (thin lines) and mean CAFs (thick dashed lines) for chirps of the post-gentamicin group to normal ranges (gray areas) constructed with the data from experiment 1. At 90 dB pSPL, the individual N_1 amplitude functions of the ten gentamicin-exposed gerbils [Fig. 10(a), thin lines] fell essentially within the normal range (mean of normalized N_1 amplitude +/− 2SD). In contrast, at 60 dB pSPL a large portion of the functions for six out of the ten gentamicin-exposed animals [Fig. 10(b), thin lines] fell outside the normal range. The mean post-gentamicin CAF at 60 dB pSPL [Fig. 10(b), thick dashed line] grows at a similar rate as the normal range; however, the post-gentamicin CAF is shifted approximately 1 mm closer to the apex than the normal range.

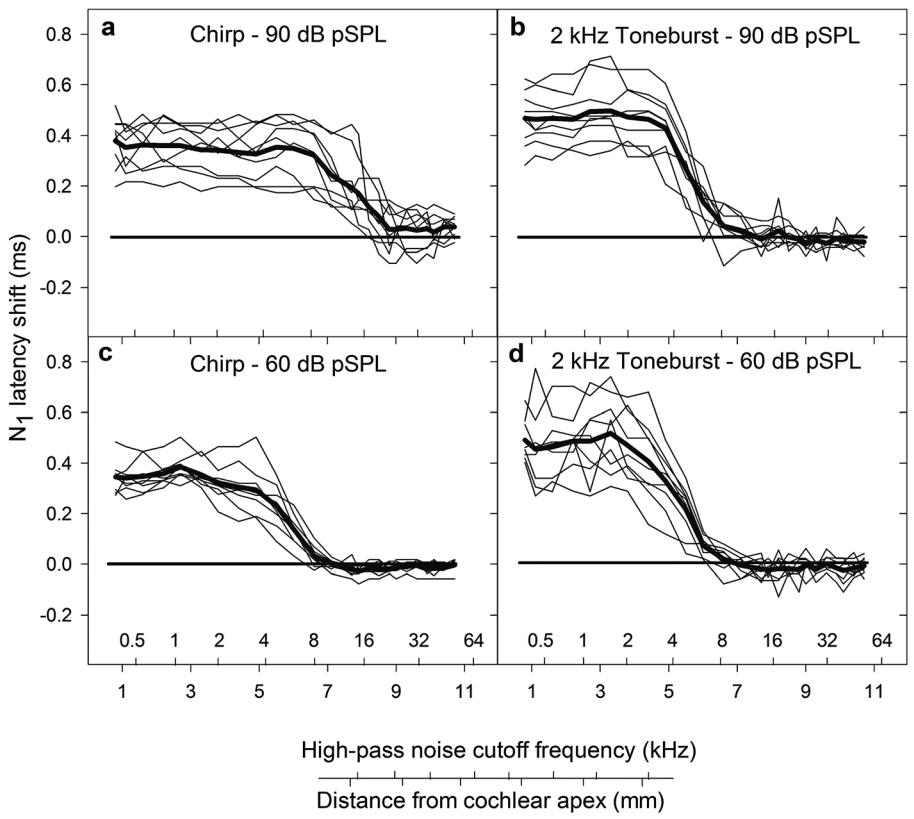

FIG. 8. N_1 latency shift (ms; masked-unmasked latency) plotted as a function of high-pass noise cutoff frequency and distance from cochlear apex for the normal-hearing group of experiment 1. Individual animal data are shown with thin lines and the group means are shown with thick lines. The latency shift functions are generally consistent with the theory suggested by Teas *et al.* (1962) that the location of synchronous neural firing for moderate and high-level stimuli is shifted toward the apex proportional to the high-pass noise cutoff frequency. The trends in latency shift resemble the inverse of the patterns observed for N_1 amplitude growth (Fig. 6).

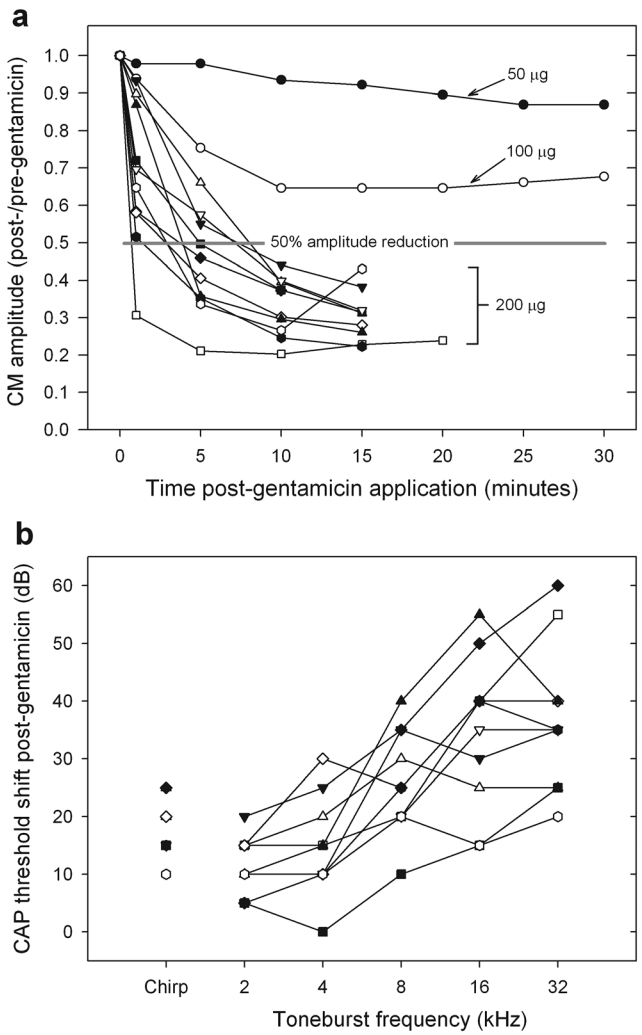

FIG. 9. (a) Cochlear microphonic (CM) data for the ten gerbils in experiment 2 indicate an exponential decrease in amplitude over a course of 15 min following application of 200 μg of gentamicin to the round window niche. The CM was evoked with 16 kHz tonebursts (10 ms in duration) at 80 dB pSPL. Dose-response curves for lower gentamicin doses (50 and 100 μg) are shown for comparison. (b) Post-gentamicin CAP threshold data show shifts ranging from 10 to 25 dB for chirps and a general trend of increasing threshold shifts for tonebursts as stimulus frequency increases.

The mean R^2 values for the CAF fits of the post-gentamicin data (0.93 for chirps at 90 dB pSPL and 0.96 for chirps at 60 dB pSPL, respectively) indicate that the sigmoid function accounts for a large majority of the variance in N_1 amplitude for both stimulus conditions. The R^2 values of the post-gentamicin CAFs for chirps at 90 dB pSPL ranged from 0.89 to 0.97. Similar to the CAF fits of the normal data for chirps at 90 B pSPL, the sigmoid parameter a had to be manually constrained for the majority of animals (9 of 10) to achieve significance for all parameters. The R^2 values for the post-gentamicin CAFs for chirps at 60 dB pSPL ranged from 0.92 to 0.98 and no manual constraints of the sigmoid parameters were necessary.

The bottom panels [(c) and (d)] of Fig. 10 compare the individual (thin lines) and mean post-gentamicin NDFs (thick dashed lines) to the normal NDF ranges (mean +/− 2SD; gray areas) established with the data from experiment 1. Similar to the N_1 amplitude plots in the upper panels, the NDFs of the two groups essentially overlap for chirps at 90 dB pSPL [Fig. 10(c)], whereas for chirps at 60 dB pSPL [Fig. 10(d)], the distributions of the two groups appear to differ. Table III summarizes the descriptive statistics and results of the independent samples t-tests of the difference across groups for mean bandwidth and mean peak location. As hypothesized, there was not a significant difference between groups for mean NDF bandwidth or mean NDF peak location for chirps at 90 dB pSPL. For chirps at 60 dB pSPL, mean NDF bandwidth was not significantly different across groups; however, the mean NDF peak location for the gentamicin-exposed group was significantly closer ($p = 0.01$) to the apex than the mean NDF peak location for the normal-hearing group (open circle). As noted in Table III, the assumption of equal variance was violated for the NDF peak location data for chirps at 60 dB pSPL. The assumption of equal variance was satisfied for the NDF bandwidth data for chirps at 60 dB pSPL and for the NDF bandwidth and peak location data for chirps at 90 dB pSPL. The assumption of normality was satisfied for the NDF bandwidth and NDF peak location data for both chirp conditions of both groups (i.e., normal and post-gentamicin) according to the Shapiro–Wilk test of normality.

3. N_1 latency shifts

Figure 11 shows N_1 latency shift (masked-unmasked latency) as a function of high-pass noise cutoff frequency across the two stimulus conditions for the ten gerbils (thin lines) in the post-gentamicin group with their respective group means (thick dashed lines). The horizontal line at zero represents the baseline N_1 latency of unmasked CAPs. Although the patterns of N_1 latency shift for the post-gentamicin group resemble the respective patterns of latency shift for the normal group, the mean shift in N_1 latency for the chirp conditions following gentamicin exposure was approximately half that of the respective chirp conditions for the normal-hearing group (Fig. 8). The latency functions of the gentamicin-exposed group (Fig. 11) also show more variability when compared to the trends of the chirp CAP latency functions of the normal-hearing group (Fig. 8).

4. Variability in NDF peak location

To determine the possible contributors to the large variability observed in the NDF peak location for chirps at 60 dB pSPL, several scatter plots were constructed and correlation analyses were performed. Figure 12 illustrates a significant negative correlation ($r = -0.74$; $p = 0.003$) between the post-gentamicin shift in NDF peak location for chirps at 60 dB pSPL and the post-gentamicin shift in chirp CAP threshold. The shift in NDF peak location was determined by calculating the differences between the individual post-gentamicin peak locations and the mean NDF peak location of the normal-hearing group for chirps at 60 dB pSPL. The individual shifts in chirp CAP threshold were determined by calculating the difference between the pre-exposure threshold and the post-exposure threshold (measured immediately following the 15-min gentamicin-exposure period). Filled circles ($n = 10$) represent the animals that met the inclusion criteria for experiment 2.

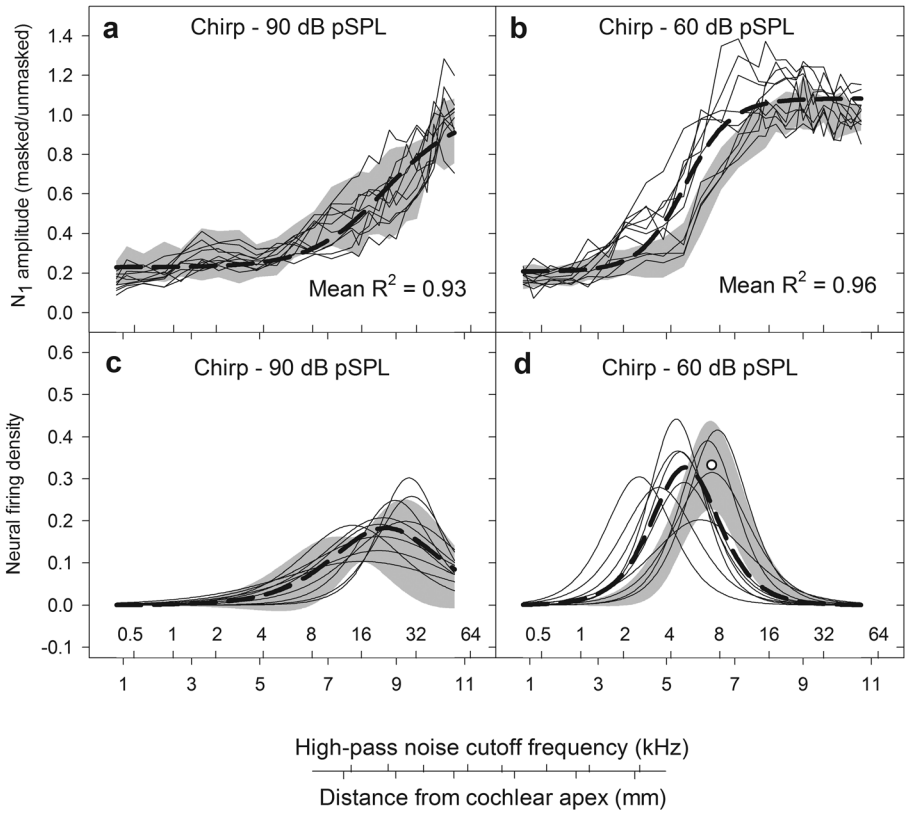

FIG. 10. (a) and (b) N_1 amplitude functions for ten gentamicin-exposed gerbils (thin lines) fall within the normal range (mean +/− 2SD; gray areas) for chirps at 90 dB pSPL, whereas for chirps at 60 dB pSPL, six out of the ten gentamicin-exposed animals fall outside the normal range. Thick dashed lines in the top panels represent the mean of the post-gentamicin CAFs. Mean R^2 values indicate that the four-parameter sigmoid function accounts for a large majority of the variance in the post-gentamicin data. (c) and (d) Individual NDFs for the ten gentamicin-exposed gerbils (thin lines) with the mean NDFs (thick dashed lines) plotted against the normal ranges (mean +/− 2SD; gray areas) indicate minimal difference between the mean bandwidth and mean peak location for chirps at 90 dB pSPL. For chirps at 60 dB pSPL, mean bandwidth did not differ across groups but the mean peak location for the gentamicin-exposed group was significantly more apical than the mean peak location for the normal-hearing group (open circle). See Table II for statistical analyses.

Open circles ($n = 4$) represent animals that were excluded from analysis due to progressive CAP threshold shifts during the course of data collection (two upper circles) or due to minimal chirp CAP threshold shifts or insufficient reduction in CM amplitude following gentamicin application (two lower circles). Other scatter plots between the shift in NDF peak location for chirps at 60 dB pSPL and other post-gentamicin measures including toneburst CAP threshold shift and CM amplitude reduction did not reveal any significant correlations.

TABLE III. Descriptive statistics and results of independent samples *t*-tests comparing bandwidth and peak location of chirp NDFs for normal to post-gentamicin (post-gent.) groups at 90 and 60 dB pSPL (experiment 2)

Chirp—90 dB pSPL						
	Bandwidth (mm)			Peak location (mm)		
	Mean	SD	*p*	Mean	SD	*p*
Normal[a]	4.56	0.66	0.64	8.43	0.79	0.46
Post-gent.	4.86	1.53		8.68	0.58	
Chirp—60 dB pSPL						
	Bandwidth (mm)			Peak location (mm)		
	Mean	SD	*p*	Mean	SD	*p*
Normal	2.78	0.39	0.24	6.28	0.17	0.01[b]
Post-gent.	3.05	0.54		5.55	0.72	

[a]Sample size of normal group reduced to 7 for Chirp 90 due to exclusion of two outliers (initial masked amplitude > 2 SD above the mean initial masked amplitude of all chirp conditions).
[b]Equal variances not assumed per Levene's Test. SD: standard deviation of the mean.

IV. DISCUSSION

The objectives of this study were to use the high-pass masking technique to establish normative ranges for CAP-derived neural density functions using broadband chirps and 2 kHz tonebursts, and to determine if high-level NDFs are unaltered by OHC pathology. The results support the central hypothesis that high-level NDFs are independent of OHC pathology while moderate-level NDFs are influenced by OHC pathology. Other observations relating to chirp CAP amplitude, the design of the chirp stimulus, an alternative analysis method, and the high-pass masking paradigm have implications for future studies and clinical application.

A. Experiment 1: NDF differences across stimulus type

The results of experiment 1 indicate that high-level chirps result in broader NDF bandwidths than high-level low frequency tonebursts suggesting that high-level chirps evoke a broader spread of neural firing along the cochlear partition than high-level low frequency (2 kHz) tonebursts. On average, the NDF bandwidths for chirps at 90 dB pSPL [Fig. 7(a)] were 1.5 times broader and peaked nearly 2 mm closer to the base of the cochlea than those for 2 kHz tonebursts at 90 dB pSPL [Fig. 7(b)]. The NDF bandwidth comparison across stimulus type for the moderate level of 60 dB pSPL suggests that moderate-level 2 kHz tonebursts [Fig. 7(d)] evoke a larger spread of neural firing than moderate-level chirps [Fig. 7(c)]. However, the bandwidth of the NDFs for 2 kHz tonebursts at 60 dB pSPL was highly variable. The NDF peak location for 2 kHz tonebursts at 60 dB pSPL was also considerably more variable than for chirps at 60 dB

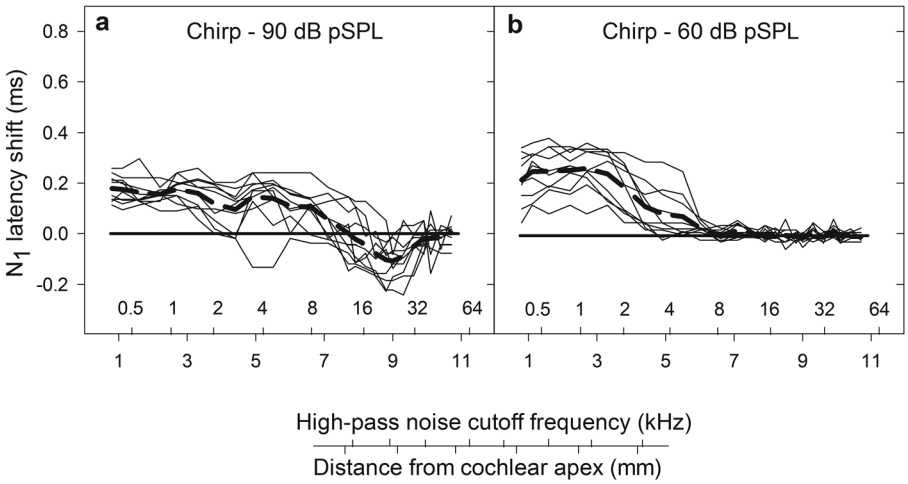

FIG. 11. N_1 latency shift (ms; masked-unmasked latency) plotted as a function of high-pass noise cutoff frequency and distance from cochlear apex for the post-gentamicin group in experiment 2 (thin lines = individual animal data; thick dashed lines = group means). Post-gentamicin latency shifts were approximately half that of the chirp conditions for the normal-hearing group (Fig. 7).

pSPL, but the mean data suggest that the distribution of neural firing evoked by moderate-level chirps peaks significantly closer to the base than for moderate-level low frequency tonebursts.

B. Experiment 2: NDF comparisons across groups

The negligible differences between high-level NDFs for the normal-hearing and gentamicin-exposed groups [Fig. 10(c)] support the hypothesis that gentamicin-induced OHC pathology does not significantly alter the spread of neural firing evoked with high-level chirp stimuli. The secondary observation that the peak location of moderate-level NDFs for gentamicin-exposed animals was shifted significantly closer to the cochlear apex than the NDF peak location for normal hearing animals [Fig. 10(d)] suggests that the pattern of neural firing evoked by moderate-level chirps is influenced by OHC pathology. The direction of the shift in peak location (i.e., toward the apex) for post-gentamicin NDFs is consistent with pathology/dysfunction of basal OHCs. In other words, without functioning OHCs in the basal region of the cochlea, the distribution of neural firing for moderate-level chirps shifts apically to cochlear regions in which OHCs are functional. The apical shift in neural firing may be enhanced by the relative location of the round-window electrode that is no longer dominated by basal activity if basal OHCs are dysfunctional. Together, the patterns observed for high-level and moderate-level NDFs are consistent with previous studies (e.g., Dallos and Harris, 1978; Ruggero and Rich,1991; Fridberger *et al.*, 2002) suggesting that OHCs act primarily to amplify basilar membrane displacement for low to moderate-level inputs.

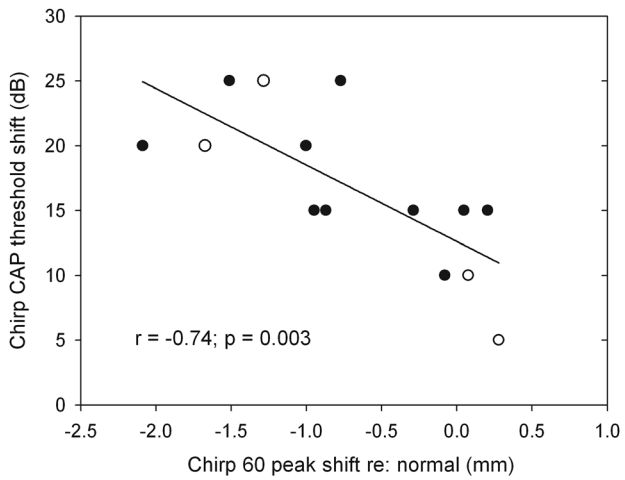

FIG. 12. Plotting the post-gentamicin shift in chirp CAP thresholds against the post-gentamicin shift in NDF peak location for chirps at 60 dB pSPL (re: normal mean peak location for chirps at 60 dB pSPL) reveals a significant inverse correlation between the two variables. Negative values for peak shift indicate apical shifts re: normal peak location. Filled circles ($n = 10$) represent the animals that met the inclusion criteria for experiment 2. Open circles ($n = 4$) represent animals that were excluded from analysis due to progressive CAP threshold shifts during the course of data collection (two upper circles) or due to minimal chirp CAP threshold shifts following gentamicin application (two lower circles).

Despite receiving the same 200 μg dose of gentamicin, the peak location of post-gentamicin NDFs for chirps at 60 dB pSPL [Fig. 10(d)] varied by as much as 2 mm across animals. This observation suggests inter-animal differences in gentamicin susceptibility that are consistent with the results of Wanamaker *et al.* (1998) indicating differing amounts of hair cell damage in gerbils receiving equivalent transtympanic doses of gentamicin. The significant negative correlation ($r = -0.74$; $p = 0.003$) between the shift in peak location for moderate-level NDFs and chirp CAP threshold shift (Fig. 12) suggests that chirp CAP threshold shifts may predict the extent of gentamicin-induced shifts in neural firing evoked with moderate-level stimuli.

C. Unmasked CAP amplitudes

Chirp CAP waveforms were considerably larger in amplitude and had narrower N_1 morphology than 2 kHz toneburst CAPs (Fig. 5). These observations suggest that broadband chirps generate synchronous neural firing across a larger number of auditory neurons than 2 kHz tonebursts even at high-levels. Figure 5 also illustrates that, on average, chirps at 90 dB pSPL yield smaller CAP amplitudes than chirps at 60 dB pSPL. This finding may be related to the design of the chirp used in this study. Specifically, the chirp stimulus was constructed based on N_1 latency data for near-threshold toneburst CAPs and the instantaneous frequency was not adjusted to account for differences in the traveling wave velocity across different signal levels (Fobel and Dau,

2004). Dau *et al*. (2000) also held constant the instantaneous frequency of their chirp stimulus across level and observed a similar roll-off in wave-V amplitude of ABRs evoked with high-level chirps.

D. Chirp stimulus

As mentioned above, the instantaneous frequency, and therefore the duration, of the chirp stimulus used in this study was held constant for both stimulus levels (i.e., 60 and 90 dB pSPL). In addition to being smaller in amplitude than chirp CAPs at 60 dB pSPL, chirp CAPs at 90 dB pSPL [e.g., Fig. 3(a)] also had broader N_1 morphology than CAPs at 60 dB pSPL [e.g., Fig. 5(b)]. Generation of level-specific chirps with different cochlear delay models, as suggested by Cebulla and Elberling (2010), Elberling *et al*. (2010), and Elberling and Don (2010) may further optimize the temporal synchrony achieved with high-level chirps.

E. Alternative analysis technique

Taking the analytical derivative of the four-parameter sigmoid function [Eq. (2)] that was used to fit the N_1 amplitude growth data imposes a Gaussian-like distribution on the NDFs. However, this fitting approach misses the subtle fluctuations in the normalized CAP amplitude data (e.g., Figs. 6 and 10) and would be inadequate to describe a bimodal distribution of neural firing density for a cochlea with a gap of missing fibers (e.g., Fig. 1). An alternative analysis method that would preserve the "fine-structure" of neural firing involves plotting the numerical derivative of the normalized CAP amplitude data (Fig. 13).

Comparing the numeric NDFs (Fig. 13, thin lines) to the corresponding analytic NDFs (Fig. 13, thick lines) reveals that analytic NDFs correspond closely with the numeric NDFs for all stimulus conditions except for chirps at 90 dB pSPL [Fig. 13(a)]. The mean analytic NDF for chirps at 90 dB pSPL suggests that neural firing density accumulates gradually beginning at approximately 3 mm from cochlear apex. The mean numeric NDF, however, indicates a tri-modal distribution that includes a small rise in neural firing density between 1 and 3 mm from cochlear apex. The most prominent peak of the tri-modal numeric NDF for chirps at 90 dB pSPL occurs at approximately 10 mm from the apex suggesting that peak firing density is nearly 2 mm closer to the base than suggested by the analytic NDF (8.22 mm from apex). The tri-modal distribution of the numeric NDF for high-level chirps may be related to asynchronous neural firing triggered by upward spread of excitation (Elberling *et al*., 2010). Designing a high-level chirp with a low-level basilar membrane delay function, as was done in this study, could also increase the potential for less than optimal temporal synchronization of neural firing.

As is evident in Fig. 13, all of the numeric NDFs, except for the NDF for chirps at 90 dB pSPL, closely resemble the corresponding analytic NDF (i.e., a Gaussian function). However, given a stimulus that theoretically generates broad, in-phase displacements of the basilar membrane (e.g., high-level chirps and high-level low frequency tonebursts) and uniform auditory neuron density along the length of the gerbil cochlea (Keithley *et al*., 1989), a linear increase in neural firing density would be expected. Two possible explanations for the "band-limited" nature of the NDFs obtained in this study relate to the mode of stimulus presentation and the spectral characteristics of the stimuli. First, the acoustic stimuli were presented via a loudspeaker in free-field without compensating for the resonance of the gerbil ear canal. A mid-frequency resonance in the ear canal could have given dominance to the mid-frequency region of the basilar membrane. Second, the spectrum of the chirp used in this study [Fig. 2(c)] was designed to be relatively flat from 1 to 60 kHz, spanning nearly the entire frequency range of gerbil hearing. To compensate for the reduced gerbil-hearing sensitivity for low and high frequencies and achieve equal weighting on the basilar membrane, the spectral energy for low and high frequencies would need to be increased relative to the energy for mid-frequencies (e.g., Shore and Nuttall, 1985). Shaping the chirp stimulus in this manner could also have the unintended effect of increasing the upward spread of masking that would lead to asynchronous neural firing.

F. High-pass noise masking paradigm

Similar to the high-pass noise masking paradigms used in previous studies (Teas *et al*., 1962; Elberling, 1974; Eggermont, 1976; Spoor *et al*., 1976; Zerlin and Naunton, 1976; Evans and Elberling, 1982; Shore and Nuttall, 1985), the masking paradigm used in this study led to decreases in N_1 amplitude and increases in N_1 latency as the high-pass noise cutoff frequency decreased [e.g., Fig. 3(b)]. The masking paradigms of previous studies have generally included 6–8 high-pass cutoff frequencies representing octave intervals (e.g., Teas *et al*., 1962) with one exception: the study in guinea pig by Shore and Nuttall (1985) used 18 cutoff frequencies representing 1/3 octave intervals between 0.4 and 20 kHz. The masking paradigm used in the current study included 25 cutoff frequencies representing 0.25 mm increments along the first 3 mm of the basal turn and 0.5 mm increments for the middle through apical regions of the gerbil cochlea (3–11 mm) providing distance-based amplitude growth functions with relatively high resolution.

Previous studies have primarily focused on calculating derived-band waveforms to infer regional cochlear contributions to the CAP and to estimate behavioral hearing thresholds. In this study, a novel technique was used to derive neural density functions from cumulative amplitude functions describing CAP amplitude growth as a function of masker cutoff frequency. Accurate interpretation of the neural density functions (e.g., peak location and bandwidth of neural firing) relies heavily on using acoustic stimuli that generate broad, in-phase displacements of the basilar membrane and synchronous neural firing throughout the majority of the cochlea (e.g., broadband chirps). Using stimuli such as clicks could produce fluctuations in CAP amplitude growth related to temporal smearing that would confound the ability of the neural density function to provide a location-specific estimate of auditory nerve survival. Even high-level chirp stimuli designed to compensate for the cochlear traveling wave delay may trigger upward spread of excitation that could result in less than optimal neural synchrony and compromise the accuracy of neural density functions.

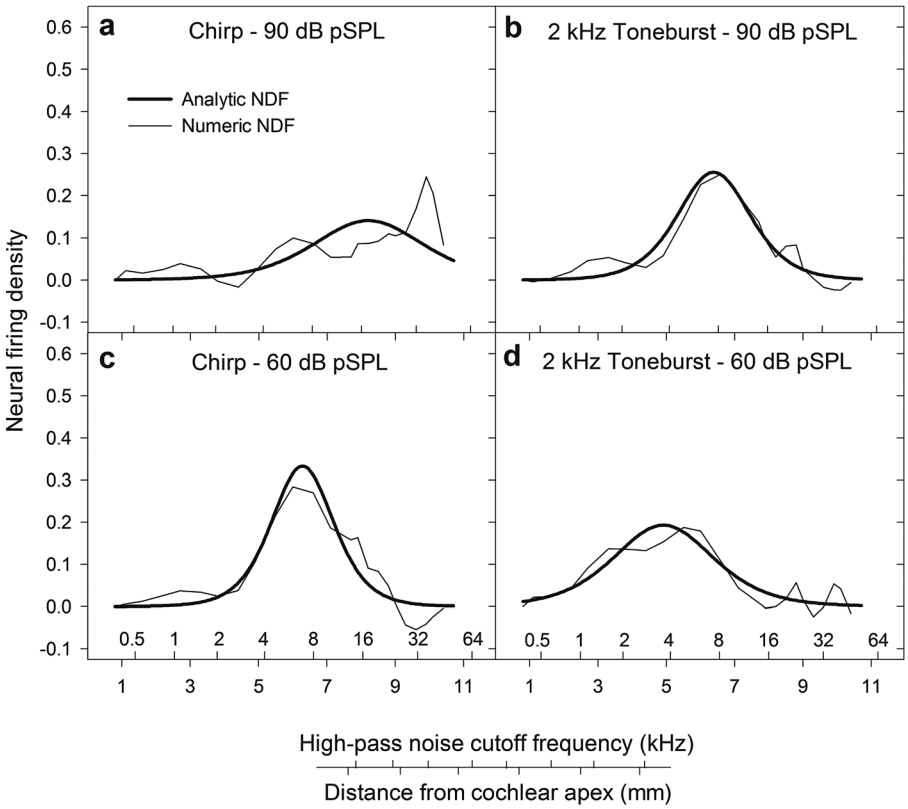

FIG. 13. An alternative method of analyzing neural firing density involves constructing numeric NDFs by calculating the numerical derivatives of the N_1 amplitude data (instead of taking the analytical derivative of the equations fitted to the data to construct analytic NDFs). These numeric NDFs (thin lines) preserve the "fine-structure" of neural firing density that may be useful for differentiation of normal and pathologic cochleae. However, other than for chirp stimuli at 90 dB pSPL (top left panel), the analytic NDFs (thick lines; mean NDFs from experiment 1) correspond closely with the distributions of neural firing depicted by the numeric NDFs.

Under-masking and over-masking might also complicate interpretation of NDFs. For example, an initial broadband masker level that reduced the unmasked CAP by 80% was chosen for this study with the goal of observing a masked CAP waveform for all 25 masking conditions. Firing among apical fibers is assumed to produce the residual 20% response. However, for a cochlea with apical nerve damage, the residual 20% of neural firing could only come from other locations wherein normal neurons are present. This issue could confound the ability of CAP amplitude growth alone to specify neural damage in the cochlear apex. Increasing the initial level of the masker to completely mask the CAP before varying the masker cutoff frequency to record partially-masked CAPs could possibly resolve that issue, but could also result in over-masking. Significant over-masking could potentially lead to CAP threshold elevations (as observed in preliminary experiments for this study) or cause fluctuations in the cumulative growth pattern of CAP amplitude that could obscure the relation between the neural density function and cochlear innervation density. Another possibility would be to include N_1 latency shift as a possible predictor variable of the damage location. Similar to the latency shifts observed for the gentamicin-exposed group, the latency-shift functions for cochleae with apical nerve damage may be lower than normal because there is a relatively shorter distance between the cochlear place dominating the unmasked response (e.g., base) and the cochlear place dominating the residual 20% response (e.g., middle).

V. CONCLUSIONS

The results of this study indicate that high-level chirps trigger a broader spread of synchronous neural firing along the cochlear partition than high-level low frequency tonebursts suggesting that chirps are superior stimuli for mapping auditory nerve firing density throughout the cochlea with a high-pass masking paradigm. The comparison between normal-hearing and gentamicin-exposed animals indicates that neural firing density functions derived with moderate-level chirps are altered by OHC pathology whereas those derived with high-level chirps are not, pointing to their potential utility in providing an estimate of auditory nerve survival that is independent of OHC pathology. Future research will determine the strength of correlation between high-level chirp NDFs and the anatomical distribution of surviving auditory neurons in animals with partial lesions of the auditory nerve. A strong correlation between the shape of NDFs and the extent and location of neural pathology will prompt translational research in human patients to determine if the masked-CAP approach could provide clinicians a method to account for auditory nerve survival when prescribing amplification via hearing aids, programming the stimulation characteristics of cochlear implants, or eventually, specifying the target for delivery of therapeutic agents that can promote neural regeneration.

ACKNOWLEDGMENTS

This research was funded by The Royal National Institute for Deaf People (Action on Hearing Loss), United Kingdom. The authors thank John Ferraro, Judy Widen, Tiffany Johnson, Thomas Imig, and three anonymous reviewers for their helpful comments on an earlier version of this manuscript. The authors also thank Ashlee Martz and Megan Ash for their assistance with data collection.

Al-momani, M. O., Ferraro, J. A., Gajewski, B. J., and Ator, G. (**2009**). "Improved sensitivity of electrocochleography in the diagnosis of Meniere's disease," Int. J. Audiol. **48**, 811–819.

Anderson, D. J., Rose, J. E., Hind, J. E., and Brugge, J. F. (**1971**). "Temporal position of discharges in single auditory nerve fibers within the cycle of a sine-wave stimulus: frequency and intensity effects," J. Acoust. Soc. Am. **49**, 1131–1139.

Békésy, G. v. (**1960**). *Experiments in Hearing*. (McGraw-Hill, New York), pp. 1–745.

Borg, E., and Moller, A. R. (**1975**). "Effect of central depressants on the acoustic middle ear reflex in rabbit," Acta Physiol. Scand. **94**, 327–338.

Cebulla, M., and Elberling, C. (**2010**). "Auditory brain stem responses evoked by different chirps based on different delay models," J. Am. Acad. Audiol. **21**, 452–460.

Chertoff, M. E. (**2004**). "Analytic treatment of the compound action potential: Estimating the summed post-stimulus time histogram and unit response," J. Acoust. Soc. Am. **116**, 3022–3030.

Chertoff, M. E., Lichtenhan, J. T., Tourtillott, B. M., and Esau, K. S. (**2008**). "The influence of noise exposure on the parameters of a convolution model of the compound action potential," J. Acoust. Soc. Am. **124**, 2174–2185.

Chertoff, M. E., Lichtenhan, J. T., and Willis, M. (**2010**). "Click- and chirp-evoked human compound action potentials," J. Acoust. Soc. Am. **127**, 2992–2996.

Cone-Wesson, B., Vohr, B. R., Sininger, Y. S., Widen, J. E., Folsom, R. C., Gorga, M. P., and Norton, S. J. (**2000**). "Identification of neonatal hearing impairment: Infants with hearing loss," Ear Hear. **21**, 488–507.

Dallos, P., and Harris, D. (**1978**). "Properties of auditory nerve responses in absence of outer hair cells," J. Neurophysiol. **41**, 365–383.

Dau, T., Wegner, O., Mellert, V., and Kollmeier, B. (**2000**). "Auditory brainstem responses with optimized chirp signals compensating basilar-membrane dispersion," J. Acoust. Soc. Am. **107**, 1530–1540.

Don, M., Eggermont, J. J., and Brackmann, D. E. (**1979**). "Reconstruction of the audiogram using brain stem responses and high-pass noise masking," Ann. Otol. Rhinol. Laryngol. Suppl. **57**, 1–20.

Don, M., Kwong, B., Tanaka, C., Brackmann, D., and Nelson, R. (**2005**). "The stacked ABR: A sensitive and specific screening tool for detecting small acoustic tumors," Audiol. Neurootol. **10**, 274–290.

Don, M., Vermiglio, A. J., Ponton, C. W., Eggermont, J. J., and Masuda, A. (**1996**). "Variable effects of click polarity on auditory brain-stem response latencies: analyses of narrow-band ABRs suggest possible explanations," J. Acoust. Soc. Am. **100**, 458–466.

Earl, B. R., and Chertoff, M. E. (**2010**). "Predicting auditory nerve survival using the compound action potential," Ear Hear. **31**, 7–21.

Eggermont, J. J. (**1976**). "Analysis of compound action potential responses to tone bursts in the human and guinea pig cochlea," J. Acoust. Soc. Am. **60**, 1132–1139.

Eggermont, J. J. (**1977**). "Compound action potential tuning curves in normal and pathological human ears," J. Acoust. Soc. Am. **62**, 1247–1251.

Eggermont, J. J., Spoor, A., and Odenthal, D. W. (**1976**). "Frequency specificity of tone-burst electrocochleography," in *Electrocochleography*, edited by R. J. Ruben, C. Elberling, and G. Salomon (University Park Press, Baltimore), pp. 215–246.

Elberling, C. (**1974**). "Action potentials along the cochlear partition recorded from the ear canal in man," Scand. Audiol. **3**, 13–19.

Elberling, C., Callo, J., and Don, M. (**2010**). "Evaluating auditory brainstem responses to different chirp stimuli at three levels of stimulation," J. Acoust. Soc. Am. **128**, 215–223.

Elberling, C., and Don, M. (**2010**). "A direct approach for the design of chirp stimuli used for the recording of auditory brainstem responses," J. Acoust. Soc. Am. **128**, 2955–2964.

Evans, E. F., and Elberling, C. (**1982**). "Location-specific components of the gross cochlear action potential: an assessment of the validity of the high-pass masking technique by cochlear nerve fibre recording in the cat," Audiology **21**, 204–227.

Ferraro, J. A., and Durrant, J. D. (**2006**). "Electrocochleography in the evaluation of patients with Meniere's disease/endolymphatic hydrops," J. Am. Acad. Audiol. **17**, 45–68.

Fobel, O., and Dau, T. (**2004**). "Searching for the optimal stimulus eliciting auditory brainstem responses in humans," J. Acoust. Soc. Am. **116**, 2213–2222.

Fridberger, A., Zheng, J., Parthasarathi, A., Ren, T., and Nuttall, A. (**2002**). "Loud sound-induced changes in cochlear mechanics," J. Neurophysiol. **88**, 2341–2348.

Gibson, W. P., and Sanli, H. (**2007**). "Auditory neuropathy: An update," Ear Hear. **28**, 102S–106S.

Goldstein, M. H. J., and Kiang, N. Y. S. (**1958**). "Synchrony of neural activity in electric responses evoked by transient acoustic stimuli," J. Acoust. Soc. Am. **30**, 107–114.

Hall, R. D. (**1990**). "Estimation of surviving spiral ganglion cells in the deaf rat using the electrically evoked auditory brainstem response," Hear. Res. **45**, 123–136.

Heydt, J. L., Cunningham, L. L., Rubel, E. W., and Coltrera, M. D. (**2004**). "Round window gentamicin application: An inner ear hair cell damage protocol for the mouse," Hear. Res. **192**, 65–74.

Husmann, K. R., Morgan, A. S., Girod, D. A., and Durham, D. (**1998**). "Round window administration of gentamicin: A new method for the study of ototoxicity of cochlear hair cells," Hear. Res. **125**, 109–119.

Keithley, E. M., Ryan, A. F., and Woolf, N. K. (**1989**). "Spiral ganglion cell density in young and old gerbils," Hear. Res. **38**, 125–134.

Kujawa, S. G., and Liberman, M. C. (**2009**). "Adding insult to injury: Cochlear nerve degeneration after 'temporary' noise-induced hearing loss," J. Neurosci. **29**, 14077–14085.

Müller, M. (**1996**). "The cochlear place-frequency map of the adult and developing Mongolian gerbil," Hear. Res. **94**, 148–156.

Overstreet, E. H., Temchin, A. N., and Ruggero, M. A. (**2002**). "Basilar membrane vibrations near the round window of the gerbil cochlea," J. Assoc. Res. Otolaryngol. **3**, 351–361.

Ren, T., and Nuttall, A. L. (**2001**). "Basilar membrane vibration in the basal turn of the sensitive gerbil cochlea," Hear. Res. **151**, 48–60.

Ruggero, M. A., and Rich, N. C. (**1991**). "Furosemide alters organ of corti mechanics: Evidence for feedback of outer hair cells upon the basilar membrane," J. Neurosci. **11**, 1057–1067.

Russell, I. J., and Nilsen, K. E. (**1997**). "The location of the cochlear amplifier: Spatial representation of a single tone on the guinea pig basilar membrane," Proc. Natl. Acad. Sci. **94**, 2660–2664.

Sheppard, W. M., Wanamaker, H. H., Pack, A., Yamamoto, S., and Slepecky, N. (**2004**). "Direct round window application of gentamicin with varying delivery vehicles: A comparison of ototoxicity," Otolaryngol. Head Neck Surg. **131**, 890–896.

Shore, S. E., and Nuttall, A. L. (**1985**). "High-synchrony cochlear compound action potentials evoked by rising frequency-swept tone bursts," J. Acoust. Soc. Am. **78**, 1286–1295.

Smith, L., and Simmons, F. B. (**1983**). "Estimating eighth nerve survival by electrical stimulation," Ann. Otol. Rhinol. Laryngol. **92**, 19–23.

Spoor, A., Eggermont, J. J., and Odenthal, D. W. (**1976**). "Comparison of human and animal data concerning adaptation and masking of eight nerve compound action potential," in *Electrocochleography*, edited by R. J. Ruben, C. Elberling, and G. Salomon (University Park Press, Baltimore), pp. 183–198.

Suryadevara, A. C., Wanamaker, H. H., and Pack, A. (**2009**). "The effects of sound conditioning on gentamicin-induced vestibulocochlear toxicity in gerbils," Laryngoscope **119**, 1166–1170.

Teagle, H. F., Roush, P. A., Woodard, J. S., Hatch, D. R., Zdanski, C. J., Buss, E., and Buchman, C. A. (**2010**). "Cochlear implantation in children with auditory neuropathy spectrum disorder," Ear Hear. **31**, 325–335.

Teas, D. C., Eldridge, D. H., and Davis, H. (**1962**). "Cochlear responses to acoustic transients: An interpretation of whole-nerve action potentials," J. Acoust. Soc. Am. **34**, 1438–1459.

Wanamaker, H. H., Gruenwald, L., Damm, K. J., Ogata, Y., and Slepecky, N. (**1998**). "Dose-related vestibular and cochlear effects of transtympanic gentamicin," Am. J. Otol. **19**, 170–179.

Zerlin, S., and Naunton, R. F. (**1976**). "Effects of high-pass masking on the whole-nerve response to third-octave audiometric clicks," in *Electrocochleography*, edited by R. J. Ruben, C. Elberling, and G. Salomon (University Park Press, Baltimore), pp. 207–213.